

RESEARCH ARTICLE

 OPEN ACCESS 

Silica nanoparticles containing nano-silver and chlorhexidine to suppress *Porphyromonas gingivalis* biofilm and modulate multispecies biofilms toward healthy tendency

Lixin Fang^{a,b}, Yishuang Zhang^{a,b}, Long Cheng^{a,b}, Hao Zheng^{a,b}, Yiyi Wang^{a,b}, Lu Qin^{a,b}, Yingchun Cai^c, Lei Cheng^{d,e}, Wen Zhou^f, Fei Liu^a and Suping Wang^a

^aStomatology Center, The First Affiliated Hospital of Zhengzhou University, Zhengzhou, China; ^bThe Academy of Medical Sciences, Zhengzhou University, Zhengzhou, China; ^cDepartment of Orthopedics, The First Affiliated Hospital of Zhengzhou University, Zhengzhou, China; ^dState Key Laboratory of Oral Diseases, West China Hospital of Stomatology, National Clinical Research Center for Oral Diseases, Sichuan University, Chengdu, China; ^eDepartment of Operative Dentistry and Endodontics, West China School of Stomatology, Sichuan University, Chengdu, China; ^fSchool and Hospital of Stomatology, Fujian Key Laboratory of Oral Diseases & Fujian Provincial Engineering Research Center of Oral Biomaterial & Stomatological Key lab of Fujian College and University, Fuzhou, China

ABSTRACT

Objectives: This research first investigated the effect of mesoporous silica nanoparticles (nMS) carrying chlorhexidine and silver (nMS-nAg-Chx) on periodontitis-related biofilms. This study aimed to investigate (1) the antibacterial activity on *Porphyromonas gingivalis* (*P. gingivalis*) biofilm; (2) the suppressing effect on virulence of *P. gingivalis* biofilm; (3) the regulating effect on periodontitis-related multispecies biofilm.

Methods: Silver nanoparticles (nAg) and chlorhexidine (Chx) were co-loaded into nMS to form nMS-nAg-Chx. Inhibitory zone test and minimum inhibitory concentration (MIC) against *P. gingivalis* were tested. Growth curves, crystal violet (CV) staining, live/dead staining and scanning electron microscopy (SEM) observation were performed. Biofilm virulence was assessed. The 3-(4,5-dimethylthiazol-2-yl)-2,5-diphenyl tetrazolium bromide (MTT) assay and Quantitative Real Time-PCR (qPCR) were performed to validate the activity and composition changes of multispecies biofilm (*P. gingivalis*, *Streptococcus gordonii* and *Streptococcus sanguinis*).

Results: nMS-nAg-Chx inhibited *P. gingivalis* biofilm dose-dependently ($p < 0.05$), with MIC of 18.75 $\mu\text{g/mL}$. There were fewer live bacteria, less biomass and less virulence in nMS-nAg-Chx groups ($p < 0.05$). nMS-nAg-Chx inhibited and modified periodontitis-related biofilms. The proportion of pathogenic bacteria decreased from 16.08 to 1.07% and that of helpful bacteria increased from 82.65 to 94.31% in 25 $\mu\text{g/mL}$ nMS-nAg-Chx group for 72 h.

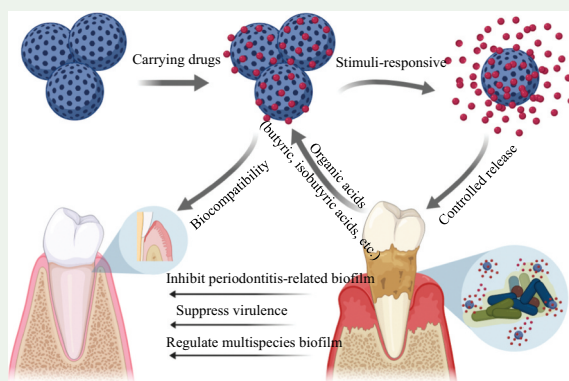
Conclusions: nMS-nAg-Chx inhibited *P. gingivalis* growth, decreased biofilm virulence and modulated periodontitis-related multispecies biofilms toward healthy tendency. pH-sensitive nMS-nAg-Chx inhibit the pathogens and regulate oral microecology, showing great potential in periodontitis adjunctive therapy.

ARTICLE HISTORY

Received 19 September 2023
Revised 20 April 2024
Accepted 23 May 2024

KEYWORDS

Mesoporous silica nanoparticles; drug delivery system; *Porphyromonas gingivalis*; antibacterial; antibiofilm; periodontitis; endotoxin; multispecies biofilm



Graphical abstract: The pH-sensitive nMS-nAg-Chx with good biocompatibility, bactericidal efficiency, and modulating ability to induce periodontitis-related biofilms toward healthy tendency

CONTACT Suping Wang  wangsupingdent@163.com  Stomatology Center, The First Affiliated Hospital of Zhengzhou University, University North Street 45, Zhengzhou, Henan 450052, China; Wen Zhou  zhouwendentist@139.com  School and Hospital of Stomatology, Fujian Key Laboratory of Oral Diseases & Fujian Provincial Engineering Research Center of Oral Biomaterial & Stomatological Key lab of Fujian College and University, Fujian Medical University, Fuzhou, Fujian 350002, China; Fei Liu  liufeidentist@163.com

© 2024 The Author(s). Published by Informa UK Limited, trading as Taylor & Francis Group.

This is an Open Access article distributed under the terms of the Creative Commons Attribution-NonCommercial License (<http://creativecommons.org/licenses/by-nc/4.0/>), which permits unrestricted non-commercial use, distribution, and reproduction in any medium, provided the original work is properly cited. The terms on which this article has been published allow the posting of the Accepted Manuscript in a repository by the author(s) or with their consent.

Introduction

Periodontitis is one of the most prevalent chronic oral diseases caused by dysbiosis of oral microecology, leading to tooth loss in adults [1,2]. The prevalence of periodontitis ranges from 31 to 76% reported by European and United States studies [3]. Severe forms of this disease affect 11% of the global population [4]. *P. gingivalis* is the dominant pathogen in the subgingival dental plaque, which can produce virulence factors in periodontal pockets and trigger a destructive change in the periodontium [5]. Their colonies establish in the oral epithelium and produce endotoxins to interact with toll-like receptors [6–9]. Lipopolysaccharide (LPS), also termed endotoxin, is an integral structural component of the outer membrane of *P. gingivalis* [10]. The presence of *P. gingivalis* is related to the recurrence or aggravation of periodontitis after periodontal treatment [11]. Therefore, periodontal treatment needs to reduce the *P. gingivalis* prevalence or eradicate the adherence to the infected root surfaces of periodontitis-related biofilms.

Subgingival scaling and root planning are conventional periodontitis therapies to remove subgingival dental plaques. However, mechanical debridement fails to remove the lingering bacteria in deep periodontal pockets and surface irregularity areas. Local drug therapies have focused on chlorhexidine (Chx) mouthwash to eliminate the remaining germs after subgingival curettage. However, Chx oral administration for a long period may bring in mitochondrial damage and oral equilibrium imbalance.

Incorporating Chx into a drug delivery system, capable of allowing a wide spacing of dosage for sustained release and enhanced biosafety, is mandatory to eliminate the aforementioned shortcomings [12–14]. Furthermore, antibiotics combination, a new alternative strategy to reduce resistance emergence, has been widely developed and applied in the field of dentistry. Chx and silver nanoparticles (nAg) have been successfully used for synergistic antibacterial and employed as antimicrobial-releasing agents to be incorporated in dental materials [15–19]. nAg killed microbiota through several mechanisms, which further guaranteed a lower risk of bacterial resistance of combined application [20,21]. However, problems with the biosafety of nAg remain. Previous *in vitro* and *in vivo* studies have reported that nAg and non-coated nAg showed cytotoxicity toward different cell lines [22,23]. Besides, biofilm microenvironments prevent antimicrobial diffusion through the deeper layers of the matrix, which reduces the activity of potent agents [24]. nMS have been applied as the carrier to deliver drugs into microorganisms and improve antimicrobial

performance, which encapsulate agents and target specific tissue to keep a sustained drug concentration in lesion [25–29].

According to previous studies [30–32], silica nanoparticles containing nano-silver and chlorhexidine (nMS-nAg-Chx) were synthesized successfully by our research group, which respond to acids and showed better compatibility. To investigate the release behavior of this antiseptic, nMS-nAg-Chx were dispersed in simulated body fluid solutions (pH = 4.0, 5.5, 7.4) in our previous study [33]. Results showed Chx release in nMS-nAg-Chx was triggered by acid stimuli, and the cumulative release amount of nMS-nAg-Chx in (pH = 4.0) was tripled by that in neutral (pH = 7.4). The releasing amount of nMS-nAg-Chx became preferentially accelerated in acid conditions (pH = 4.0, 5.5). Furthermore, this new antiseptic was also equipped with sustained release for carboxylate functional groups that were introduced to the frameworks, which could be protonated and dissociated in acidic environments [30–32]. The cumulative agent release in nMS-nAg-Chx had an initial burst in the first 20 h and continually released more than 100 h [33]. Compared with the burst release in the first 10 h of inorganic nMS, the hydrophobic framework composed of carbon materials and organically modified hybrids realizes sustained release [30,31,34]. Biocompatibility was also tested in our previous report [33]. The cytotoxicity of high-purified Chx (<99%, free Chx) and 20% chlorhexidine gluconate solution (CHG) was measured to compare with nMS-nAg-Chx. nMS-nAg-Chx exhibited lower cytotoxicity against human lung adenocarcinoma cells (A549), human umbilical vein endothelial cells (HUVECs), human gingival fibroblasts (HGF) and oral squamous cancer cells (OSCC), which was in line with the slow-release behavior in the neutral environment. Most importantly, cell viability remained at 80% even when the concentration of nMS-nAg-Chx suspension was at 57.8 µg/mL.

To date, no research has been done to determine whether the nMS-nAg-Chx can inhibit *P. gingivalis* growth and virulence. As the polymicrobial synergy between functional microorganisms and pathogenic bacteria has arisen broad attention [35–39], this research selected three central strains which have important implications for the periodontitis process. This periodontitis-associated multispecies biofilm was used to investigate community transition during the nMS-nAg-Chx treatment period [40–42]. Previous studies reported an acidic microenvironment containing peptides and heme-derivatives facilitates the selective expansion of periodontitis-promoting microorganisms, mainly *P. gingivalis*

[43,44]. nMS-nAg-Chx would destroy the beneficial conditions for periodontitis-promoting bacterial growth for the preferential release in an acid micro-environment [31,45,46].

Therefore, the objectives of this study were to investigate (1) the inhibitory effect on *P. gingivalis* biofilm; (2) the influence on endotoxins production of *P. gingivalis* biofilm; (3) the suppressing and modulating effect on multispecies biofilm for the first time. It was hypothesized that (1) culture medium containing nMS-nAg-Chx would effectively suppress *P. gingivalis* growth; (2) nMS-nAg-Chx would reduce the virulence of *P. gingivalis* biofilm; (3) periodontitis-related multispecies biofilms would be inhibited and modulated towards healthy tendency with nMS-nAg-Chx intervention.

Materials and Methods

Preparation of nMS-nAg-Chx

nMS-nAg-Chx was obtained commercially (Ruixi Biological Technology, Xian, China), which was synthesized via a method reported by Lu et al. [30,31]. Briefly, 1.5 g of cetyltrimethylammonium tosylate mixed with 0.5 g of triethanolamine was dissolved in 100 mL of deionized water and stirred at 80°C for 1 h. Then, quickly added 1.0 g of Tetraethyl orthosilicate, 1.0 g of bis(3-triethoxysilylpropyl)disulfide and 0.2 g of 3-aminopropyltriethoxysilane. The synthesized NH₂-nMS were collected and washed three times with ethanol. The silver-decorated nMS were prepared according to previous studies [30,31]. About 9.0 mL of 5% AgNO₃ solution and 1 mL of ammonium hydroxide (28%) were mixed and then reacted with NH₂-nMS in the dark under ultrasonication. Centrifuged nAg-nMS and washed three times with deionized water. Carboxylate group-functionalized nAg-nMS (COOH-nAg-nMS) were prepared to load Chx to achieve pH sensitivity. Preparing Chx solution (5 mg/mL) by dissolving 25 mg of Chx in 5 mL of ethanol and added 5 mL of COOH-nAg-nMS (10 mg/mL). The mixture was stirred at room temperature for 24 h.

Bacterial strains and biofilm formation

Streptococcus gordonii (*S. gordonii*) strain ATCC 10558 and *Streptococcus sanguinis* (*S. sanguinis*) strain ATCC 10556 were cultured in brain-heart infusion (BHI) medium. *P. gingivalis* strain ATCC 33,277 was cultured in BHI medium supplemented with hemin (5 µg/mL) and vitamin K (0.5 µg/mL). All of these strains were cultured at 37°C under anaerobic conditions (80% N₂, 10% CO₂ and 10% H₂) for 24 h [47]. Culture media containing nMS-nAg-Chx of 6.25 µg/mL, 12.5 µg/mL, 18.75 µg/mL and 25 µg/mL

were prepared. Sterilized frosted glass slides were placed at the bottom of 24-well plates, and 1 mL of the above medium was added to each well. Bacterial suspensions were adjusted to 1 × 10⁹ CFU/mL. Then, the suspensions were blended in a ratio of 1:1:1, and 30 µL of mixed bacterial solution was added to each well. The multispecies biofilms of 48 h and 72 h were cultured anaerobically at 37°C. The culture medium was changed every 24 h.

Effect of nMS-nAg-Chx on *Porphyromonas gingivalis* biofilm

Inhibition zone test

Circular filter paper with a diameter of 10 mm and thickness of 0.7 mm was placed gently in the middle of the agar medium according to previous studies. Forty microliters of nMS-nAg-Chx in 50 µg/mL and 25 µg/mL was impregnated into the circular filter paper. Two hundred microliters of the bacterial suspension cultivated overnight was diluted to 10⁷ CFU/mL and swabbed uniformly across an agar plate with a diameter of 90 mm and a thickness of 4 mm. After incubating at 37°C for 24 h, the antibacterial property was demonstrated by the appearance of the inhabitation zone. All experiments were conducted in at least three replicates.

MIC

MIC is the minimum concentration of an antimicrobial agent to completely inhibit bacteria growth. The MIC of nMS-nAg-Chx against *P. gingivalis* biofilm was determined by a two-fold serial dilution method on a 96-well plate [48]. nMS-nAg-Chx was dispersed in sterile distilled water and diluted with a BHI solution to prepare the starting concentrations (150 µg/mL). Ten microliters of standard bacterial suspension was mixed with the above culture media containing nMS-nAg-Chx on a 96-well plate. BHI solution without agents served as the negative control group. BHI solution without bacteria served as positive control. All experiments were conducted in at least three replicates in sextuplicate.

Bacterial growth curve

Culture media containing nMS-nAg-Chx was diluted to 25 µg/mL, 18.75 µg/mL, 12.5 µg/mL, 6.25 µg/mL and 3.125 µg/mL. The bacterial suspension was diluted with PBS to prepare an inoculum (1 × 10⁸ CFU/mL). Bacteria were inoculated in 200 µL of BHI containing the above five concentrations of nMS-nAg-Chx in 96-well plates. Cultured anaerobically at 37°C for 100 h. BHI solution served as the positive control. The growth of *P. gingivalis* was monitored at 0 h, 3 h, 6 h, 9 h, 12 h, 15 h, 18 h, 24 h, 30 h, 36 h, 42 h and 48 h by measuring and recording the OD600 values of each well using Multi-Mode

Microplate Reader [49]. All experiments were conducted in at least three replicates in sextuplicate.

CV staining

The biofilms attached to the frosted glass slides ($n = 6$) were gently rinsed 3 times with PBS to wash away planktonic bacteria. Transferred these slides to a new 96-well plate and incubated biofilms with 200 μL 0.01% CV solution for 1 h at 37°C anaerobically. Stained biofilms were treated with 30% acetic acid for 5 min. The absorbance was detected at 590 nm according to previous studies [50]. All experiments were conducted at least three replicates in sextuplicate.

SEM observation

P. gingivalis biofilms were cultured anaerobically with nMS-nAg-Chx suspension in the 24-well plate at 37°C for 48 h and 72 h. The culture media was changed each 24 h. The 2-day and 3-day biofilms were gently washed three times with PBS to remove planktonic bacteria and fixed in 2.5% glutaraldehyde (LEAGENE, Beijing, China) at 4°C overnight. Then, dehydrated using graded ethanol and coated with a gold-sputter. The biomass and structure of biofilms were visualized by SEM observation. All experiments were conducted in at least three replicates in sextuplicate.

Live/dead bacteria staining

The frosted glasses attached to biofilms were washed three times with distilled water to remove planktonic bacteria. Transferred these slides to a new 24-well plate and stained biofilms using the BacLight live/dead bacterial viability kit (Molecular Probes, Eugene, OR, USA). The disks with 48 h and 72 h biofilms were examined by CLSM. The group cultured in BHI solution without nMS-nAg-Chx served as a control. Living bacteria were stained green and dead bacteria were stained red. Then, we counted the total amount of bacteria in the visual fields and further calculated the ratio of live to dead bacteria to demonstrate the significant killing effect of nMS-nAg-Chx. All experiments were conducted in at least three replicates in sextuplicate.

Effect of nMS-nAg-Chx on virulence of *Porphyromonas gingivalis* biofilm

LPS staining

The biofilms attached to the frosted glasses were placed gently on the new 24-well plated. All glasses were rinsed with distilled water to remove planktonic bacteria. Then, biofilms were stained with 5 μL of iFluor® 555-Concanavalin A conjugate (2 mg/mL),

and images were observed using CLSM. LPS would produce red fluorescence. The group cultured in BHI solution without nMS-nAg-Chx served as a control. All experiments were conducted in at least three replicates in sextuplicate.

Endotoxin detection

End-point Chromogenic Lyophilized Amebocyte Lysate (LAL kits, Xiamen Bioendo Technology, Co., Ltd., China) was used for endotoxin detection. Bacterial standard endotoxins were dissolved in endotoxin-free water and diluted for the standard curve. The culture supernatant fluid of all samples was collected. One hundred microliters of supernatant was added to an endotoxin-free tube and mixed with 100 μL of Limulus reagent. In the presence of endotoxins, the factors in LAL kits were activated in a proteolytic cascade that result in the cleavage of a colorless artificial peptide substrate [51]. Operated according to the operation manual and measured the absorbance at 545 nm. All experiments were conducted in at least three replicates in sextuplicate.

Effect of nMS-nAg-Chx on multispecies biofilm

MTT assay

The biofilms attached to the frosted glass slides ($n = 6$) were gently rinsed 3 times with PBS to wash away planktonic bacteria. Transferred these slides to a new 96-well plate and incubated biofilms with 1 mL MTT dye (0.5 mg/mL in PBS) for 1 h at 37°C to form formazan crystals anaerobically. The samples were then transferred to new 24-well plates filled with 1 mL of dimethyl sulfoxide (DMSO) to solubilize the formazan crystals. Shaking plates gently for 20 min at room temperature. The absorbance was detected at 540 nm [52]. All experiments were conducted in at least three replicates in sextuplicate.

qPCR

Total DNA of biofilms was isolated by lysozyme buffer (Vazyme, Nanjing, China). DNA concentrations were detected by NanoDrop 2000 spectrophotometer (Thermo Scientific, Waltham, MA, USA). qPCR was carried out in sextuplicate for each gene with 2 μL of cDNA by using Premix Ex Taq™ (Takara, Kyoto, Japan) in 20 μL reaction volume according to the instruction. qPCR was performed by the ABI StepOnePlus (Thermo Fisher, CA, USA) [53]. Plotted standard curves and calculated respective contents of three strains in multispecies biofilms. All experiments were conducted in at least three replicates in sextuplicate.

Gene Name	Primer Name	Primer sequence (5'-3')	5'	3'
<i>Streptococcus gordonii</i>	<i>S. gordonii-F</i>	GGAAGTAATCTTCGACAATCCTATTATAC		
	<i>S. gordonii-R</i>	CTCATCACCGTTTCATGGTAGC		
	<i>S. gordonii-probe</i>	TGGAAGATATAACCGTGAAG	FAM	MGB
<i>Streptococcus sanguis</i>	<i>S. sanguis-F</i>	TCAGCCRCCAATCTATGGTGT		
	<i>S. sanguis-R</i>	GCTTGGAGCGACCTTCACTGTA		
	<i>S. sanguis-probe</i>	AGGTCGGAAAGTGAAGTC	FAM	MGB
<i>Porphyromonas gingivalis</i>	<i>p.gingivalis-F</i>	ACGGATAAACGAACGCTCAAG		
	<i>p.gingivalis-R</i>	CGGACAAACTCCTTCAATCCTC		
	<i>p.gingivalis-probe</i>	ACGGCAGTGGCTATAA	FAM	MGB

Results

Preparation of nMS-nAg-Chx

The morphology results of nMS-nAg-Chx were observed by transmission electron microscope, which are shown in Figure 1 a and b. NMS-nAg-Chx was spherical nanoparticle with radial channels with 17.3% Chx carrying rate, and the content of nAg in nMS-nAg-Chx was 3.8 mg/mL. The average of nMS-nAg-Chx diameter was 188 ± 6.5 nm, and nAg of 2–5 nm in size were homogeneously distributed on its surface. The BET surface area, zeta potential and polydispersity index of nMS-nAg-Chx were $516.9 \text{ m}^2/\text{g}$, $15.7 \pm 1.6 \text{ mV}$ and 0.17 ± 0.05 , respectively. Furthermore, our previous study showed that the preferential Chx release was triggered by acid stimuli (pH = 4.0), the cumulative release amount of which was tripled by that at pH = 7.4 [33].

Effect of nMS-nAg-Chx on *P. gingivalis* biofilm

Inhibition zone test

Figure 1 shows the results of the inhibition zone test. nMS-nAg-Chx inhibited *P. gingivalis* growth dose-dependently. There were obvious antibacterial zones

around the circular filter papers penetrated by nMS-nAg-Chx (Figure 1c, d). The higher the drug concentration was, the larger the inhibition zone appeared. No inhibition zone appeared in the control medium (Figure 1e). The MIC of nMS-nAg-Chx was $18.75 \mu\text{g}/\text{mL}$, which had a megascopic inhibitory effect on *P. gingivalis* growth (Figure 2 a).

Growth curve

Figure 2 b shows the growth curves of *P. gingivalis* cultured with different concentrations of nMS-nAg-Chx suspension. The growth curve of the lower concentration that $6.25 \mu\text{g}/\text{mL}$ was aligned roughly with the control group without nMS-nAg-Chx treatment. Furthermore, the logarithmic growth period of *P. gingivalis* began at approximately 9–15 h, but was delayed with the increase of nMS-nAg-Chx concentration. *P. gingivalis* was inhibited completely when the concentration of the drug was up to $18.75 \mu\text{g}/\text{mL}$ and $25 \mu\text{g}/\text{mL}$.

CV staining

CV staining was used to measure the *P. gingivalis* biofilm. There was a significant difference between the control groups and nMS-nAg-Chx groups, showing an obvious dose-dependent decrease in biomass

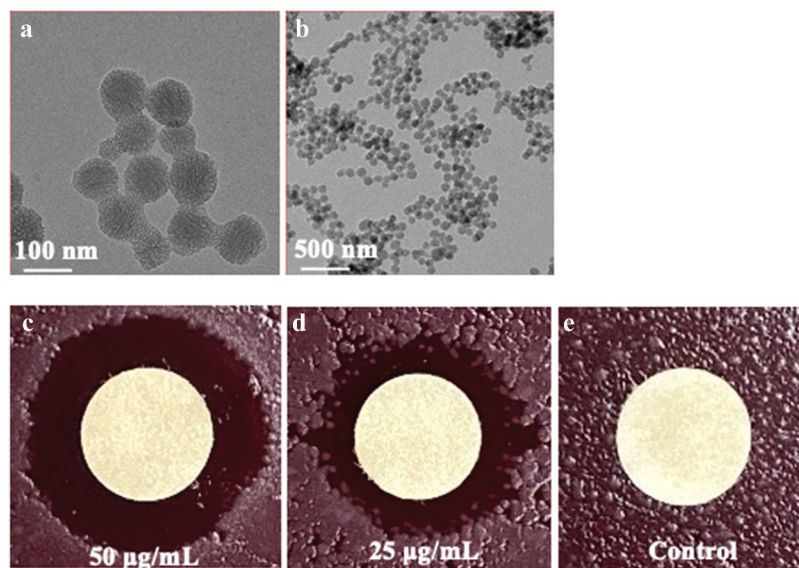


Figure 1. (a) Transmission electron microscope images of nMS-nAg-Chx at 100 nm. (b) Transmission electron microscope images of nMS-nAg-Chx at 500 nm. (c, d) Inhibition zone of nMS-nAg-Chx against *Porphyromonas gingivalis*. (e) Control group without nMS-nAg-Chx.

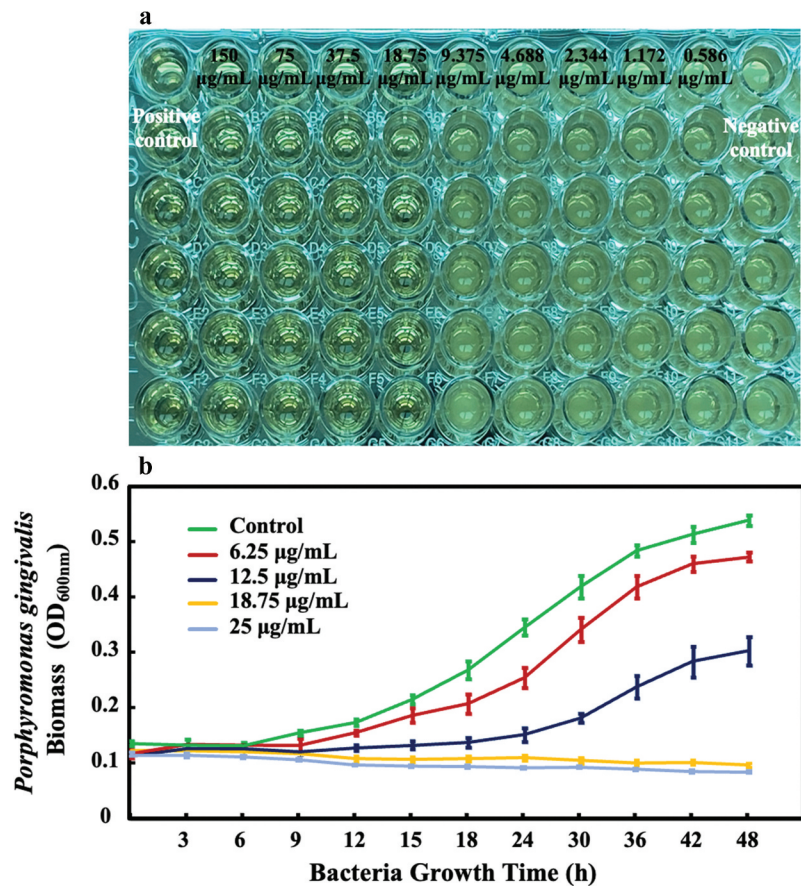


Figure 2. (a) Result graph of MIC. (b) Growth curve of *Porphyromonas gingivalis* exposed to different concentrations of nMS-nAg-Chx suspension for 48 h (mean \pm sd; n = 6).

($p < 0.05$) (Figure 3a). Meanwhile, both 48 h and 72 h *P. gingivalis* biofilms were completely inhibited at a concentration of 25 $\mu\text{g/mL}$. No significant difference was observed between the 6.25 $\mu\text{g/mL}$ group and the control group in 72 h biofilm. This may be explained by the transient biofilm suppression of nMS-nAg-Chx at 6.25 $\mu\text{g/mL}$, indicating the lower the concentration of nMS-nAg-Chx, the shorter the antibacterial period.

SEM observation

The morphological features of *P. gingivalis* biofilm were observed to detect the antibiofilm effect of nMS-nAg-Chx (Figure 3). The biomass was decreased in a dose-dependent way, and *P. gingivalis* biofilm scarcely formed especially when the concentration was up to 25 $\mu\text{g/mL}$. In addition, biofilm structures of nMS-nAg-Chx groups changed from dense to sparse, which means nMS-nAg-Chx promotes *P. gingivalis* biofilm dissociation.

Live/dead bacteria staining

The live/dead staining showed that nMS-nAg-Chx influenced bacterial vitality (Figure 4). These images indicate that *P. gingivalis* biofilm biomass was reduced. Sparser bacteria appeared in the presence of a higher concentration of nMS-nAg-Chx

(Figure 4c), and no obvious bacteria were observed in the 48 h and 72 h biofilms (Figure 4d, h). The biofilm vitality was almost suppressed significantly ($p < 0.05$), especially when the culture medium contained 25 $\mu\text{g/mL}$ of nMS-nAg-Chx (Figure 4i). There was no significant difference between control and 6.25 $\mu\text{g/mL}$ group of 72 h, which may be largely due to the dose-dependent suppressing effect and sustained-release manner. The dead bacteria ratio increased substantially when nMS-nAg-Chx concentration rose (Figure 4j). There were almost no residual bacteria in the 25 $\mu\text{g/mL}$ group, and it is hard to observe directly, so the ratio of live to dead bacteria in higher concentration groups showed large fluctuations.

Effect of nMS-nAg-Chx on virulence of *P. gingivalis* biofilm

LPS staining

The distributions of bacteria and LPS in the 48 h and 72 h biofilms in the different groups are shown in Figure 5. The control groups both cultured for 48 h and 72 h (Figure 5a, e) were covered by live bacteria and LPS. When the culture medium contains 12.5 $\mu\text{g/mL}$ of nMS-nAg-Chx, fewer bacteria and LPS were stained (Figure 5c, g). About 25 $\mu\text{g/mL}$ of nMS-nAg-

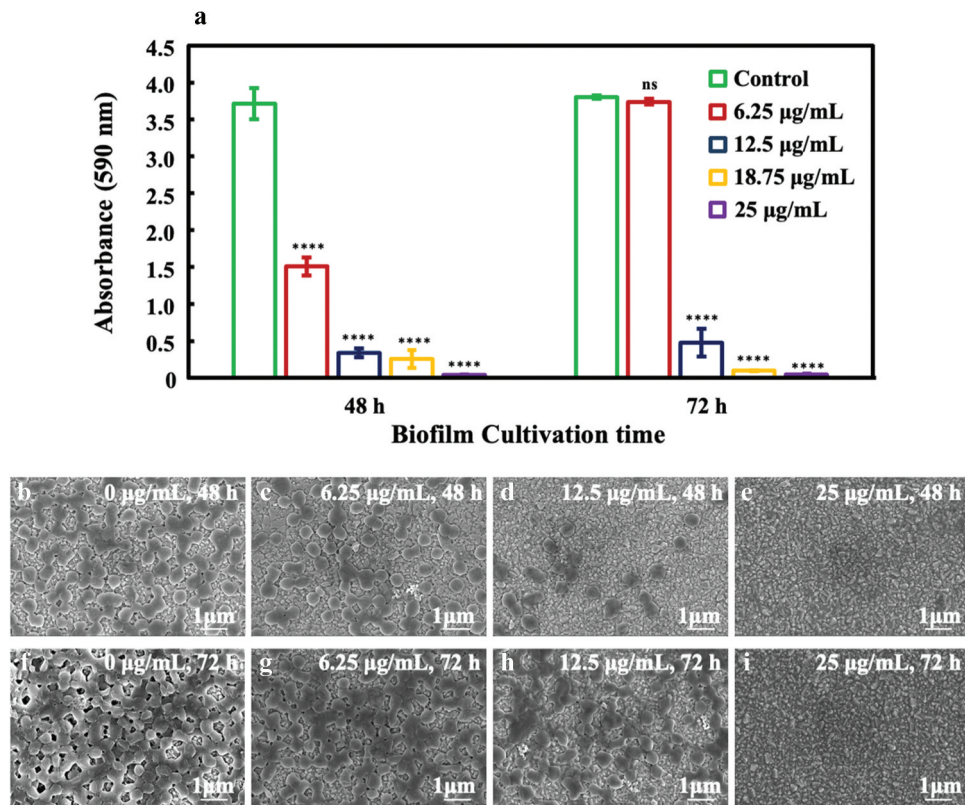


Figure 3. (a) Absorbance of *Porphyromonas gingivalis* biofilms after crystal violet staining (mean \pm sd; $n = 6$). (* $p < 0.05$). SEM images of biofilms treated by culture media containing nMS-nAg-Chx for 48 h (b, c, d, e) and 72 h (f, g, h, i) ($n = 3$).

Chx could inhibit *P. gingivalis* biofilms completely. The reduction in the amount of LPS was due to the dose-dependently suppressed effect of nMS-nAg-Chx on *P. gingivalis* biofilms growth.

Endotoxin analysis

The virulence of *P. gingivalis* was revealed by an endotoxin assay as shown in Figure 5i. Endotoxin of *P. gingivalis* from a culture medium containing nMS-nAg-Chx decreased significantly and remarkably lower than those of BHI solution ($p < 0.05$). nMS-nAg-Chx showed a dose-dependent suppression on *P. gingivalis* virulence. Endotoxin production in the control group for 72 h was 13,049.03 EU/mL, which was twice that of 6.25 µg/mL nMS-nAg-Chx suspension. In 25 µg/mL nMS-nAg-Chx group, no obvious virulence was detected.

Effect of nMS-nAg-Chx on multispecies biofilm

MTT assay

MTT assay revealed the metabolic activity of *P. gingivalis* biofilm and showed that nMS-nAg-Chx affected biofilm formation concentration dependently (Figure 6 a). The metabolic activity of the experimental groups reduced significantly compared with the control group ($p < 0.05$). Bacterial metabolism showed a declining tendency after 72 h, meaning that nMS-nAg-Chx had relatively long-lasting antibacterial capacity.

qPCR

Compared with the control group, *P. gingivalis* proliferated slowly in nMS-nAg-Chx groups (Figure 6b, c). It is worth mentioning that the percentage of *S. gordonii* and *S. sanguinis* in multispecies biofilm increased after nMS-nAg-Chx was added. The percentage of *P. gingivalis* in multispecies biofilm decreased from 16.08 to 1.07% after being cultured with 25 µg/mL of nMS-nAg-Chx for 48 h, and this reduced tendency was also present in that group of 72 h. The percentage of benign bacteria was also upregulated in nMS-nAg-Chx groups.

Discussion

The present study developed nMS-nAg-Chx to investigate the inhibitory effect on periodontitis-related pathogens for the first time. The hypotheses were proven that adding nMS-nAg-Chx in culture medium suppressed the proliferation and virulence of *P. gingivalis* biofilm. In addition, nMS-nAg-Chx inhibited periodontal multispecies biofilms and upgraded the composition of benign bacteria, inducing biofilms towards a healthy tendency.

Periodontitis sequential therapy, which involves non-surgical therapy and surgical therapy, cannot eliminate periodontal microorganisms completely due to their robust potential to invade gingival epithelium and connective tissue. Hence, concerted

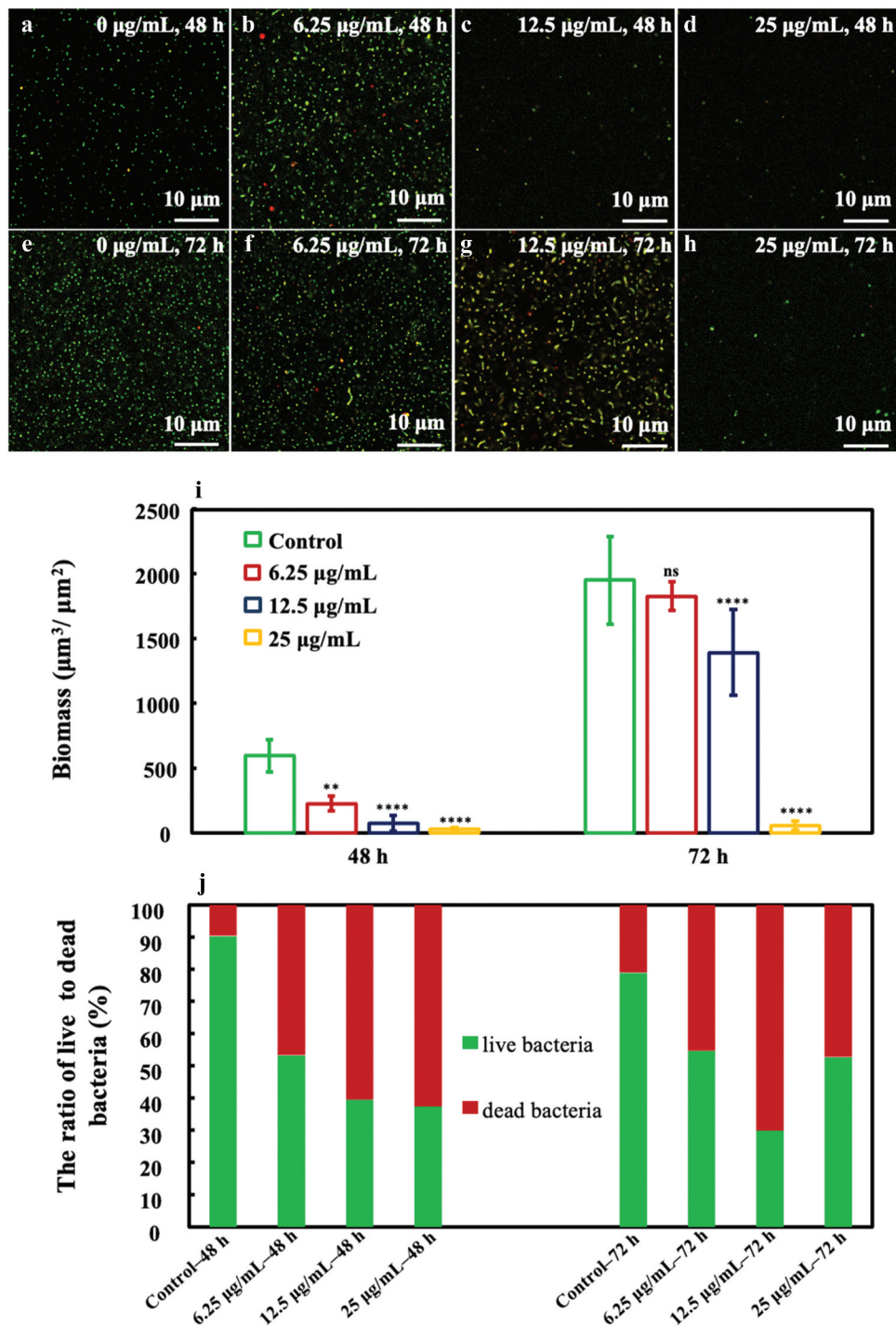


Figure 4. Live/dead bacterial staining images of biofilms treated with culture media containing nMS-nAg-Chx for 48 h (a, b, c, d) and 72 h (e, f, g, h). Live bacteria were stained green and dead bacteria were stained red. (i) Biomass. (j) The ratio of live to dead bacteria (mean \pm sd; $n = 6$). (* $p < 0.05$).

efforts must be made to consider the origin of this disease and treat it with appropriate agents as an adjunct to standard mechanical therapy [54]. The desired adjuvant drug after supragingival scaling and subgingival curettage should be little thrill to the inflamed periodontium. nMS had several advantages including releasing drugs in a controlled fashion, sustaining drug concentration for a prolonged period and avoiding any irritation to the tissues. Drug-loaded nMS unleashed antiseptics continually and delicately to target sites, which would be

beneficial for biomedical applications in the field of periodontitis.

Modified nMS could deliver drugs into microorganisms and target specific tissue for the responsive release [25–29]. This study loaded Chx and nAg on the nMS surface or inside the pores (nMS-nAg-Chx), which received synergistic antibacterial effects, providing a potential strategy for drug resistance of Chx long-term use. Meanwhile, the neurotoxicity of nAg overdose still hinders its more widespread application. Its biocompatibility is enhanced after being

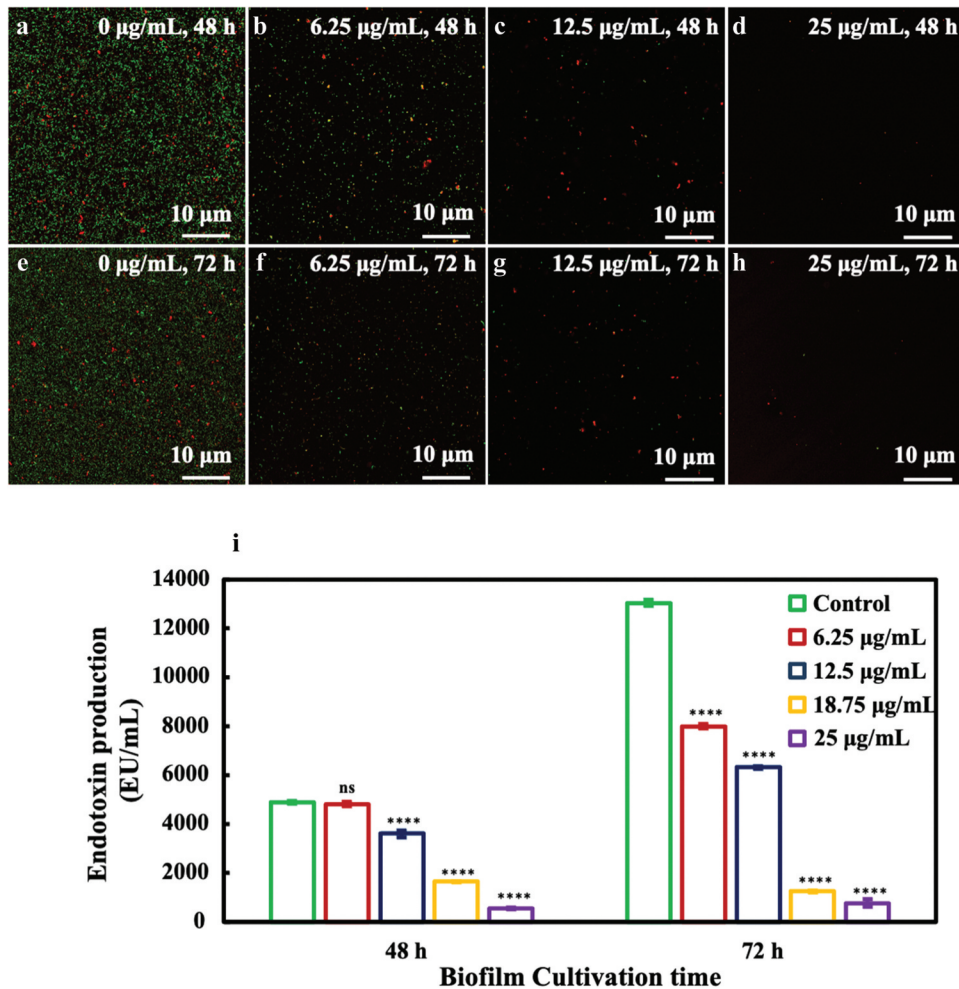


Figure 5. LPS staining images of biofilms treated with culture media containing nMS-nAg-Chx for 48 h (a, b, c, d) and 72 h (e, f, g, h). Bacteria were stained green and LPS were stained red ($n = 3$). (I) Endotoxin production of *Porphyromonas gingivalis* biofilms for 48 h and 72 h (mean \pm sd; $n = 6$). (* $p < 0.05$).

encapsulated inside nMS. Previous studies evaluated the influence of nMS-nAg-Chx on the viability of different cell types [30,31,33]. All results demonstrated that nMS-nAg-Chx with less cytotoxicity, compared with Chx, nAg and CHG gargle, did not exhibit side effects even *in vivo*. Most importantly, nMS-nAg-Chx with acid responsibility could target infectious sites to sterilize specifically, avoiding the oral equilibrium imbalance. Placing nMS-nAg-Chx directly in subgingival sites makes active drug release possible to combat microbial attacks in a sustained or controlled way [54]. Thus, compared with Chx or nAg alone, nMS-nAg-Chx exhibited better antibacterial efficiency and biocompatibility, showing less risk of drug resistance with sustained release.

Periodontitis and periodontal treatments often lead to a gingival recession which exposes roots to the oral environment and raises the risk of root caries [55]. Previous research showed that pH-sensitive nMS-nAg-Chx effectively killed cariogenic bacteria [30]. *P. gingivalis* biofilm model had been widely used in several previous studies to research periodontitis [56,57]. *P. gingivalis* elevated the virulence of

periodontal biofilm by undermining host defenses, changing the makeup of the biofilm community and facilitating a rise in overall bacterial burden [58]. Eick et al. cultured *P. gingivalis* for 48 h and yielded a mature biofilm structure [59,60]. In the present study, periodontitis-related biofilms were cultured for 48 h and 72 h to verify the antibacterial effect of nMS-nAg-Chx. Results confirmed that nMS-nAg-Chx suppressed *P. gingivalis* biofilm proliferation and endotoxin production in a dose-dependent manner. nMS-nAg-Chx delayed the start of the logarithmic growth period gradually as concentrations increased. About 18.75 $\mu\text{g/mL}$ of nMS-nAg-Chx could inhibit *P. gingivalis* growth totally for 48 h. When *P. gingivalis* biofilms were cultured in the medium containing 18.75 $\mu\text{g/mL}$ of nMS-nAg-Chx for 72 h, endotoxin production was significantly reduced from 13,049.03 EU/mL to 1249.43 EU/mL ($p < 0.05$). This result was directly reflected in the LPS staining plots (Figure 5).

This study first investigated the influence of nMS-nAg-Chx on the periodontitis-related multispecies biofilm. Biofilm formation is microbial colonization

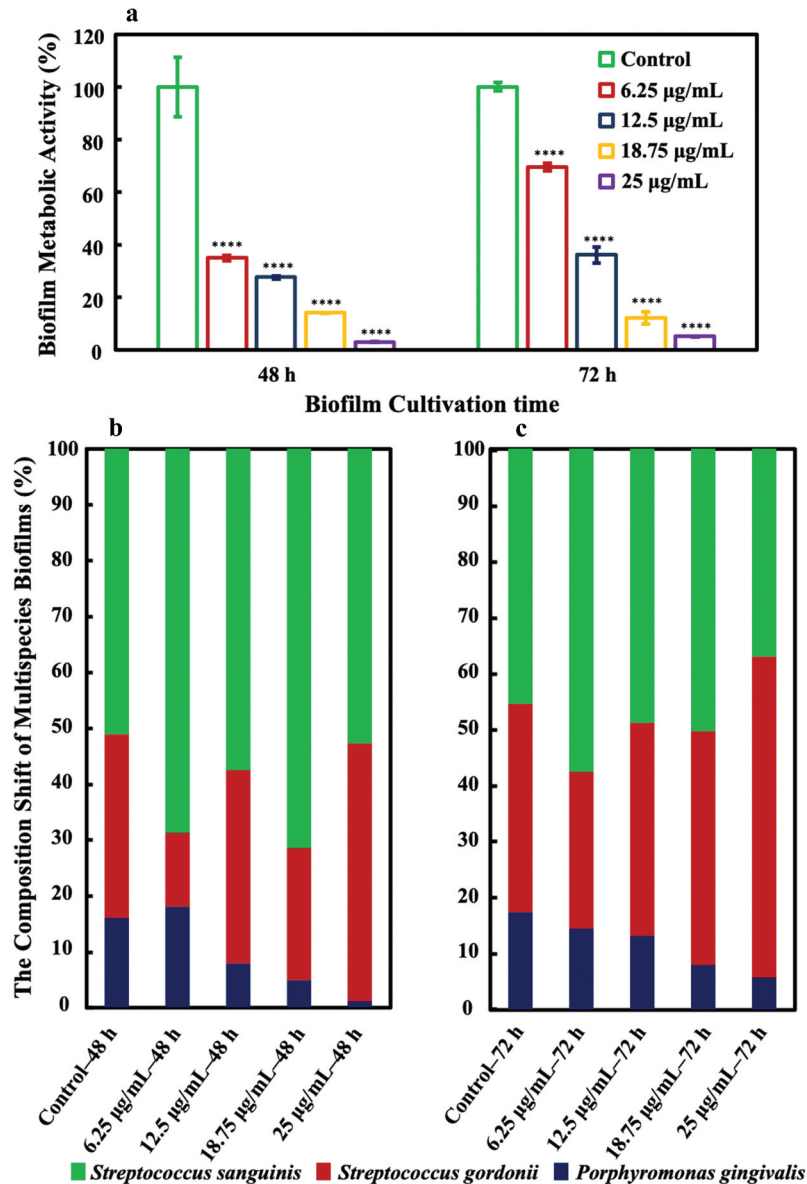


Figure 6.(a) MTT metabolic activity of multispecies biofilms for 48 h and 72 h (mean \pm sd; n = 6). (* p<0.05). The percentage of three strains in multispecies biofilm detected by qPCR. The composition shift of *Porphyromonas gingivalis*, *Streptococcus gordonii* and *Streptococcus sanguinis* in multispecies biofilm treated with nMS-nAg-Chx suspension for 48 h (b) and 72 h (c). (n = 6).

on the root surface that depends on inter-bacterial cross-feeding [58]. The occurrence of periodontitis is related to the change that a low-abundance opportunistic pathogen becomes the dominant periodontal pathogen. *P. gingivalis* is frequently detected in subgingival plaque, causing oral dysbiosis by orchestrating other microbial pathogens [61–63]. Streptococci are the early colonizers and are abundant in subgingival plaque. *S. gordonii* and *S. sanguinis* were correlated with periodontal health by diminishing the *P. gingivalis* virulence through para-aminobenzoic acid secretion [64–70]. Previous studies implicated periodontitis is associated with the loss of *S. sanguinis* colonization [71]. Given the prevalence and interactions of the aforementioned species in the progression of periodontitis, the current study focused on multispecies biofilms containing

commensal species and pathobionts to investigate community transition during the nMS-nAg-Chx treatment period. The results of qPCR indicated nMS-nAg-Chx modulated the multispecies biofilm composition towards a healthy tendency. Significantly less *P. gingivalis* was seen in the multispecies biofilms after 48 and 72 h. After treatment with 25 $\mu\text{g/mL}$ of nMS-nAg-Chx for 48 h, the percentage of *S. gordonii* and *S. sanguinis* is 98.92%, up 15.0% from the control group.

Hence, the nMS-nAg-Chx may suppress periodontitis/caries-related biofilm and tackle the limitations of conventional antibiotics for periodontal disease. nMS-nAg-Chx can be used like a mouth rinse for caries prevention, delivering the drug to remove root residual bacteria after mechanical therapy. Furthermore, this agent responds to the acid and

works in the presence of *Streptococcus mutans*, *Enterococcus faecalis* and other acid-producing bacteria. Therefore, nMS-nAg-Chx is possibly used as a gargle or endodontic irrigant to cover the shortage of current medications. Given its ability to stop reinfection and secondary caries after root therapy, more research should be done to incorporate nMS-nAg-Chx into dental compositions or root sealers. The suppressive impact of nMS-nAg-Chx on biofilms, however, was only discernible for 3 days, which poses a drawback to our study. Oral biofilms are developed over a longer period and have more complicated structures. Future research should further evaluate the effects of long-term days *in vivo*.

Conclusion

This study developed nMS-nAg-Chx and investigated its antibacterial effects on *P. gingivalis* and modulating effects on periodontitis-related multispecies biofilm for the first time. nMS-nAg-Chx showed strong antibacterial activity against *P. gingivalis* to destroy biofilm structures and reduce biomass dose-dependently. The virulence of *P. gingivalis* biofilm also declined in nMS-nAg-Chx groups. More significantly, nMS-nAg-Chx modulated multispecies biofilms towards healthy tendency by upgrading the benign bacterial content, and the proportion of *P. gingivalis* in multispecies biofilm decreased from 17.35 to 5.69% after exposed to 25 µg/mL nMS-nAg-Chx after 72 h. Therefore, nMS-nAg-Chx shows great promise as an adjuvant therapy for periodontal disease to eliminate residual periodontitis-related pathogens and prevent root caries.

Disclosure statement

No potential conflict of interest was reported by the author(s).

Funding

The study was supported by National Natural Science Foundation of China grant 81900993 (S.W); Henan Provincial Medical Science and Technology Research Project SBGJ202102162 (S.W) and LHGJ20220353 (Y.C); Henan Provincial Department of Education Key Scientific Research Project of Higher Education Institutions 22A320006 (F.L); the Key Scientific and Technological Project of Henan Province, 222102310407 (S.W) and 212102310595 (F.L).

Author Contributions

All authors have made substantial contributions to the conception and design of the study. LF, YZ and LC have been involved in data collection and data analysis. HZ, YW, LQ and YC have been involved in data interpretation. LF, YZ and SW have been involved in drafting the

manuscript. YC, LC, WZ and FL have been involved in revising it critically. LF and SW have given final approval for the version to be published.

References

- [1] Hajishengallis G. Immunomicrobial pathogenesis of periodontitis: keystones, pathobionts, and host response. *Trends Immunol.* 2014;35(1):3–11. doi: 10.1016/j.it.2013.09.001
- [2] Sun X, Wang L, Lynch CD, et al. Nanoparticles having amphiphilic silane containing Chlorin e6 with strong anti-biofilm activity against periodontitis-related pathogens. *J Dent.* 2019;81:70–84. doi: 10.1016/j.jdent.2018.12.011
- [3] Holde GE, Oscarson N, Trovik TA, et al. Periodontitis prevalence and severity in adults: a cross-sectional study in Norwegian circumpolar communities. *J Periodontol.* 2017;88(10):1012–1022. doi: 10.1902/jop.2017.170164
- [4] Kassebaum NJ, Bernabe E, Dahiya M, et al. Global burden of severe periodontitis in 1990–2010: a systematic review and meta-regression. *J Dent Res.* 2014;93(11):1045–1053. doi: 10.1177/0022034514552491
- [5] Hajishengallis G, Darveau RP, Curtis MA. The keystone-pathogen hypothesis. *Nat Rev Microbiol.* 2012;10(10):717–725. doi: 10.1038/nrmicro2873
- [6] Duran-Pinedo AE, Chen T, Teles R, et al. Community-wide transcriptome of the oral microbiome in subjects with and without periodontitis. *Isme J.* 2014;8(8):1659–1672. doi: 10.1038/ismej.2014.23
- [7] Olsen I, Singhrao SK. Importance of heterogeneity in porphyromonas gingivalis lipopolysaccharide lipid a in tissue specific inflammatory signalling. *J Oral Microbiol.* 2018;10(1):1440128. doi: 10.1080/20002297.2018.1440128
- [8] Darveau RP. Porphyromonas gingivalis neutrophil manipulation: risk factor for periodontitis? *Trends Microbiol.* 2014;22(8):428–429. doi: 10.1016/j.tim.2014.06.006
- [9] Wang HY, Lin L, Fu W, et al. Preventive effects of the novel antimicrobial peptide Nal-P-113 in a rat periodontitis model by limiting the growth of porphyromonas gingivalis and modulating IL-1β and TNF-α production. *BMC Complement Altern Med.* 2017;17(1):426. doi: 10.1186/s12906-017-1931-9
- [10] Liebers V, Bruning T, Raulf M. Occupational endotoxin exposure and health effects. *Arch Toxicol.* 2020;94(11):3629–3644. doi: 10.1007/s00204-020-02905-0
- [11] Xiao S, Wang H, Liang K, et al. Novel multifunctional nanocomposite for root caries restorations to inhibit periodontitis-related pathogens. *J Dent.* 2019;81:17–26. doi: 10.1016/j.jdent.2018.12.001
- [12] Re ACS, Bonjovanni MC, Ferreira MP, et al. Effect of an experimental formulation containing chlorhexidine on pathogenic biofilms and drug release behavior in the presence or absence of bacteria. *Pharmaceutics.* 2019;11(2):11. doi: 10.3390/pharmaceutics11020088
- [13] Cataldo Russomando A, Vogt Sionov R, Friedman M, et al. Sinonasal stent coated with slow-release varnish of chlorhexidine has sustained protection against bacterial biofilm growth in the sinonasal cavity: An

- in vitro Study. *Pharmaceutics*. 2021;13(11):1783. doi: [10.3390/pharmaceutics13111783](https://doi.org/10.3390/pharmaceutics13111783)
- [14] Al-Obaidy SSM, Greenway GM, Paunov VN. Enhanced antimicrobial action of chlorhexidine loaded in shellac nanoparticles with cationic surface functionality. *Pharmaceutics*. 2021;13(9):1389. doi: [10.3390/pharmaceutics13091389](https://doi.org/10.3390/pharmaceutics13091389)
- [15] Delaviz Y, Finer Y, Santerre JP. Biodegradation of resin composites and adhesives by oral bacteria and saliva: a rationale for new material designs that consider the clinical environment and treatment challenges. *Dent Mater*. 2014;30(1):16–32. doi: [10.1016/j.dental.2013.08.201](https://doi.org/10.1016/j.dental.2013.08.201)
- [16] Leung D, Spratt DA, Pratten J, et al. Chlorhexidine-releasing methacrylate dental composite materials. *Biomaterials*. 2005;26(34):7145–7153. doi: [10.1016/j.biomaterials.2005.05.014](https://doi.org/10.1016/j.biomaterials.2005.05.014)
- [17] Dutra-Correa M, Leite A, de Cara S, et al. Antibacterial effects and cytotoxicity of an adhesive containing low concentration of silver nanoparticles. *J Dent*. 2018;77:66–71. doi: [10.1016/j.jdent.2018.07.010](https://doi.org/10.1016/j.jdent.2018.07.010)
- [18] Zheng T, Huang X, Chen J, et al. A liquid crystalline precursor incorporating chlorhexidine acetate and silver nanoparticles for root canal disinfection. *Biomater Sci*. 2018;6(3):596–603. doi: [10.1039/C7BM00764G](https://doi.org/10.1039/C7BM00764G)
- [19] Seung J, Weir MD, Melo MAS, et al. A modified resin Sealer: physical and antibacterial properties. *J Endod*. 2018;44(10):1553–1557. doi: [10.1016/j.joen.2018.06.016](https://doi.org/10.1016/j.joen.2018.06.016)
- [20] Abdelmonem R, Younis MK, Hassan DH, et al. Formulation and characterization of chlorhexidine HCl nanoemulsion as a promising antibacterial root canal irrigant: in-vitro and ex-vivo studies. *Int J Nanomedicine*. 2019;14:4697–4708. doi: [10.2147/IJN.S204550](https://doi.org/10.2147/IJN.S204550)
- [21] Huang L, Dai T, Xuan Y, et al. Synergistic combination of chitosan acetate with nanoparticle silver as a topical antimicrobial: efficacy against bacterial burn infections. *Antimicrob Agents Chemother*. 2011;55(7):3432–3438. doi: [10.1128/AAC.01803-10](https://doi.org/10.1128/AAC.01803-10)
- [22] Akter M, Sikder MT, Rahman MM, et al. A systematic review on silver nanoparticles-induced cytotoxicity: Physicochemical properties and perspectives. *J Adv Res*. 2018;9:1–16. doi: [10.1016/j.jare.2017.10.008](https://doi.org/10.1016/j.jare.2017.10.008)
- [23] Makama S, Kloet SK, Piella J, et al. Effects of systematic variation in size and surface coating of silver nanoparticles on their in vitro toxicity to macrophage RAW 264.7 cells. *Toxicol Sci*. 2018;162(1):79–88. doi: [10.1093/toxsci/kfx228](https://doi.org/10.1093/toxsci/kfx228)
- [24] Lewis K. Riddle of biofilm resistance. *Antimicrob Agents Chemother*. 2001;45(4):999–1007. doi: [10.1128/AAC.45.4.999-1007.2001](https://doi.org/10.1128/AAC.45.4.999-1007.2001)
- [25] Zhao X, Liu C, Wang Z, et al. Synergistic pro-apoptotic effect of a cyclic RGD Peptide-conjugated magnetic mesoporous therapeutic nanosystem on hepatocellular carcinoma HepG2 Cells. *Pharmaceutics*. 2023;15(1):15. doi: [10.3390/pharmaceutics15010276](https://doi.org/10.3390/pharmaceutics15010276)
- [26] Mehmood Y, Khan IU, Shahzad Y, et al. In-vitro and in-vivo evaluation of velpatasvir-loaded mesoporous silica scaffolds. A Prospective Carrier For Drug Bioavailability Enhancement *Pharmaceutics*. 2020;12(4):12. doi: [10.3390/pharmaceutics12040307](https://doi.org/10.3390/pharmaceutics12040307)
- [27] Figari G, Goncalves JLM, Diogo HP, et al. Understanding Fenofibrate Release from Bare and Modified Mesoporous Silica Nanoparticles. *Pharmaceutics*. 2023;15(6):15. doi: [10.3390/pharmaceutics15061624](https://doi.org/10.3390/pharmaceutics15061624)
- [28] Ribeiro TC, Sabio RM, Luiz MT, et al. Curcumin-loaded mesoporous silica nanoparticles dispersed in thermo-responsive hydrogel as potential Alzheimer disease therapy. *Pharmaceutics*. 2022;14(9):14. doi: [10.3390/pharmaceutics14091976](https://doi.org/10.3390/pharmaceutics14091976)
- [29] Barui S, Cauda V. Multimodal decorations of mesoporous silica nanoparticles for improved cancer therapy. *Pharmaceutics*. 2020;12(6):12. doi: [10.3390/pharmaceutics12060527](https://doi.org/10.3390/pharmaceutics12060527)
- [30] Lu MM, Ge Y, Qiu J, et al. Redox/pH dual-controlled release of chlorhexidine and silver ions from biodegradable mesoporous silica nanoparticles against oral biofilms. *Int J Nanomedicine*. 2018;13:7697–7709. doi: [10.2147/IJN.S181168](https://doi.org/10.2147/IJN.S181168)
- [31] Lu MM, Wang QJ, Chang ZM, et al. Synergistic bactericidal activity of chlorhexidine-loaded, silver-decorated mesoporous silica nanoparticles. *Int J Nanomedicine*. 2017;12:3577–3589. doi: [10.2147/IJN.S133846](https://doi.org/10.2147/IJN.S133846)
- [32] Fang L, Zhou H, Cheng L, et al. The application of mesoporous silica nanoparticles as a drug delivery vehicle in oral disease treatment. *Front Cell Infect Microbiol*. 2023;13:1124411. doi: [10.3389/fcimb.2023.1124411](https://doi.org/10.3389/fcimb.2023.1124411)
- [33] Wang S, Fang L, Zhou H, et al. Silica nanoparticles containing nano-silver and chlorhexidine respond to pH to suppress biofilm acids and modulate biofilms toward a non-cariogenic composition. *Dent Mater*. 2024;40(2):179–189. doi: [10.1016/j.dental.2023.11.006](https://doi.org/10.1016/j.dental.2023.11.006)
- [34] Wu M, Meng Q, Chen Y, et al. Large pore-sized hollow mesoporous organosilica for redox-responsive gene delivery and synergistic cancer chemotherapy. *Adv Mater*. 2016;28(10):1963–1969. doi: [10.1002/adma.201505524](https://doi.org/10.1002/adma.201505524)
- [35] Wang L, Li C, Weir MD, et al. Novel multifunctional dental bonding agent for class-V restorations to inhibit periodontal biofilms. *RSC Adv*. 2017;7(46):29004–29014. doi: [10.1039/C6RA28711E](https://doi.org/10.1039/C6RA28711E)
- [36] Lee JH, Kim YG, Park S, et al. Phytopigment Alizarin Inhibits multispecies biofilm development by cutibacterium acnes, staphylococcus aureus, and Candida albicans. *Pharmaceutics*. 2022;14(5):14. doi: [10.3390/pharmaceutics14051047](https://doi.org/10.3390/pharmaceutics14051047)
- [37] Tanaka CJ, Rodrigues JA, Pingueiro JMS, et al. Antibacterial Activity of a bioactive tooth-coating material containing surface pre-reacted glass in a complex multispecies subgingival biofilm. *Pharmaceutics*. 2023;15(6):15. doi: [10.3390/pharmaceutics15061727](https://doi.org/10.3390/pharmaceutics15061727)
- [38] Falanga A, Maione A, La Pietra A, et al. Competitiveness during Dual-Species Biofilm Formation of Fusarium oxysporum and Candida albicans and a Novel Treatment Strategy. *Pharmaceutics*. 2022;14(6):14. doi: [10.3390/pharmaceutics14061167](https://doi.org/10.3390/pharmaceutics14061167)
- [39] Sycz Z, Wojnicz D, Tichaczek-Goska D. Does secondary plant metabolite ursolic acid exhibit antibacterial activity against uropathogenic Escherichia coli living in single- and multispecies biofilms? *Pharmaceutics*. 2022;14(8):14. doi: [10.3390/pharmaceutics14081691](https://doi.org/10.3390/pharmaceutics14081691)
- [40] Sadeq A, Risk JM, Pender N, et al. Evaluation of the co-existence of the red fluorescent plaque bacteria

- P. gingivalis* with *S. gordonii* and *S. mutans* in white spot lesion formation during orthodontic treatment. *Photodiagnosis Photodyn Ther.* 2015;12(2):232–237. doi: [10.1016/j.pdpdt.2015.03.001](https://doi.org/10.1016/j.pdpdt.2015.03.001)
- [41] Tu Y, Ling X, Chen Y, et al. Effect of *S. Mutans* and *S. Sanguinis* on growth and adhesion of *p. gingivalis* and their ability to adhere to different dental materials. *Med Sci Monit.* 2017;23:4539–5445. doi: [10.12659/MSM.904114](https://doi.org/10.12659/MSM.904114)
- [42] Cao Q, Xiao X, Tao C, et al. Efficient clearance of periodontitis pathogens by *S. gordonii* membrane-coated H₂O₂ self-supplied nanocomposites in a “Jenga” style. *Biomater Sci.* 2023;11(16):5680–5693. doi: [10.1039/D3BM00641G](https://doi.org/10.1039/D3BM00641G)
- [43] Yan N, Xu J, Liu G, et al. Penetrating macrophage-based nanoformulation for periodontitis treatment. *ACS Nano.* 2022;16(11):18253–18265. doi: [10.1021/acsnano.2c05923](https://doi.org/10.1021/acsnano.2c05923)
- [44] Lamont RJ, Koo H, Hajishengallis G. The oral microbiota: dynamic communities and host interactions. *Nat Rev Microbiol.* 2018;16(12):745–759. doi: [10.1038/s41579-018-0089-x](https://doi.org/10.1038/s41579-018-0089-x)
- [45] Garcia MT, Ward R, Goncalves NMF, et al. Susceptibility of dental caries microcosm biofilms to photodynamic therapy mediated by fotoencicine. *Pharmaceutics.* 2021;13(11):1907. doi: [10.3390/pharmaceutics13111907](https://doi.org/10.3390/pharmaceutics13111907)
- [46] Velazquez-Moreno S, Gonzalez-Amaro AM, Aragon-Pina A, et al. Use of a cellulase from *trichoderma reesei* as an adjuvant for *enterococcus faecalis* biofilm disruption in combination with antibiotics as an alternative treatment in secondary endodontic infection. *Pharmaceutics.* 2023;15(3):15. doi: [10.3390/pharmaceutics15031010](https://doi.org/10.3390/pharmaceutics15031010)
- [47] He Z, Jiang W, Jiang Y, et al. Anti-biofilm activities of coumarin as quorum sensing inhibitor for *porphyromonas gingivalis*. *J Oral Microbiol.* 2022;14(1):2055523. doi: [10.1080/20002297.2022.2055523](https://doi.org/10.1080/20002297.2022.2055523)
- [48] Tiwari SK, Wang S, Huang Y, et al. Starvation survival and biofilm formation under subminimum inhibitory concentration of QAMs. *Biomed Res Int.* 2021;2021:8461245. doi: [10.1155/2021/8461245](https://doi.org/10.1155/2021/8461245)
- [49] Guan C, Che F, Zhou H, et al. Effect of rubusoside, a natural sucrose substitute, on *streptococcus mutans* biofilm cariogenic potential and virulence gene expression in vitro. *Appl Environ Microbiol.* 2020;86(16). doi: [10.1128/AEM.01012-20](https://doi.org/10.1128/AEM.01012-20)
- [50] Yin M, Li N, Zhang L, et al. Pseudolaric acid B ameliorates fungal keratitis progression by suppressing inflammation and reducing fungal load. *ACS Infect Dis.* 2023;9(6):1196–1205. doi: [10.1021/acsinfec.2c00536](https://doi.org/10.1021/acsinfec.2c00536)
- [51] Liu CM, Shyu YC, Pei SC, et al. In vitro effect of laser irradiation on cementum-bound endotoxin isolated from periodontally diseased roots. *J Periodontol.* 2002;73(11):1260–1266. doi: [10.1902/jop.2002.73.11.1260](https://doi.org/10.1902/jop.2002.73.11.1260)
- [52] Chen Y, Yang B, Cheng L, et al. Novel giomers incorporated with antibacterial quaternary ammonium monomers to inhibit secondary caries. *Pathogens.* 2022;11(5):11. doi: [10.3390/pathogens11050578](https://doi.org/10.3390/pathogens11050578)
- [53] Zhou Y, Wang S, Zhou X, et al. Short-time antibacterial effects of dimethylaminododecyl methacrylate on oral multispecies biofilm in vitro. *Biomed Res Int.* 2019;2019:1–10. doi: [10.1155/2019/6393470](https://doi.org/10.1155/2019/6393470)
- [54] Rr H, Dhamecha D, Jagwani S, et al. Local drug delivery systems in the management of periodontitis: A scientific review. *J Control Release.* 2019;307:393–409. doi: [10.1016/j.jconrel.2019.06.038](https://doi.org/10.1016/j.jconrel.2019.06.038)
- [55] Wang L, Melo MA, Weir MD, et al. Novel bioactive nanocomposite for class-V restorations to inhibit periodontitis-related pathogens. *Dent Mater.* 2016;32(12):e351–e61. doi: [10.1016/j.dental.2016.09.023](https://doi.org/10.1016/j.dental.2016.09.023)
- [56] Kojima T, Yasui S, Ishikawa I. Distribution of *porphyromonas gingivalis* in adult periodontitis patients. *J Periodontol.* 1993;64(12):1231–1237. doi: [10.1902/jop.1993.64.12.1231](https://doi.org/10.1902/jop.1993.64.12.1231)
- [57] Jia L, Han N, Du J, et al. Pathogenesis of Important virulence factors of *porphyromonas gingivalis* via toll-like receptors. *Front Cell Infect Microbiol.* 2019;9:262. doi: [10.3389/fcimb.2019.00262](https://doi.org/10.3389/fcimb.2019.00262)
- [58] Sakanaka A, Takeuchi H, Kuboniwa M, et al. Dual lifestyle of *Porphyromonas gingivalis* in biofilm and gingival cells. *Microb Pathog.* 2016;94:42–47. doi: [10.1016/j.micpath.2015.10.003](https://doi.org/10.1016/j.micpath.2015.10.003)
- [59] Eick S, Seltmann T, Pfister W. Efficacy of antibiotics to strains of periodontopathogenic bacteria within a single species biofilm – an in vitro study. *J Clin Periodontol.* 2004;31(5):376–383. doi: [10.1111/j.0303-6979.2004.00490.x](https://doi.org/10.1111/j.0303-6979.2004.00490.x)
- [60] Liang G, Shi H, Qi Y, et al. Specific anti-biofilm activity of carbon quantum dots by destroying *p. gingivalis* biofilm related genes. *Int J Nanomedicine.* 2020;15:5473–5489. doi: [10.2147/IJN.S253416](https://doi.org/10.2147/IJN.S253416)
- [61] Kumar PS, Griffen AL, Moeschberger ML, et al. Identification of candidate periodontal pathogens and beneficial species by quantitative 16S clonal analysis. *J Clin Microbiol.* 2005;43(8):3944–3955. doi: [10.1128/JCM.43.8.3944-3955.2005](https://doi.org/10.1128/JCM.43.8.3944-3955.2005)
- [62] Wang L, Xie X, Imazato S, et al. A protein-repellent and antibacterial nanocomposite for Class-V restorations to inhibit periodontitis-related pathogens. *Mater Sci Eng C Mater Biol Appl.* 2016;67:702–710. doi: [10.1016/j.msec.2016.05.080](https://doi.org/10.1016/j.msec.2016.05.080)
- [63] Hajishengallis G, Lamont RJ. Beyond the red complex and into more complexity: the polymicrobial synergy and dysbiosis (PSD) model of periodontal disease etiology. *Mol Oral Microbiol.* 2012;27(6):409–419. doi: [10.1111/j.2041-1014.2012.00663.x](https://doi.org/10.1111/j.2041-1014.2012.00663.x)
- [64] Kolenbrander PE, Andersen RN, Blehert DS, et al. Communication among oral bacteria. *Microbiol Mol Biol Rev.* 2002;66(3):486–505. table of contents. doi: [10.1128/MMBR.66.3.486-505.2002](https://doi.org/10.1128/MMBR.66.3.486-505.2002)
- [65] Sakanaka A, Kuboniwa M, Shimma S, et al. *Fusobacterium nucleatum* metabolically integrates commensals and pathogens in oral biofilms. *mSystems.* 2022;7(4):e0017022. doi: [10.1128/msystems.00170-22](https://doi.org/10.1128/msystems.00170-22)
- [66] Lamont RJ, El-Sabaeny A, Park Y, et al. Role of the *Streptococcus gordonii* SspB protein in the development of *porphyromonas gingivalis* biofilms on streptococcal substrates. *Microbiology (Reading).* 2002;148(6):1627–1636. doi: [10.1099/00221287-148-6-1627](https://doi.org/10.1099/00221287-148-6-1627)
- [67] Park Y, Simionato MR, Sekiya K, et al. Short fimbriae of *porphyromonas gingivalis* and their role in

- cohesion with streptococcus gordonii. *Infect Immun.* 2005;73(7):3983–3989. doi: [10.1128/IAI.73.7.3983-3989.2005](https://doi.org/10.1128/IAI.73.7.3983-3989.2005)
- [68] Redanz U, Redanz S, Treerat P, et al. Differential response of oral mucosal and gingival cells to *Corynebacterium durum*, *streptococcus sanguinis*, and *porphyromonas gingivalis* multispecies biofilms. *Front Cell Infect Microbiol.* 2021;11:686479. doi: [10.3389/fcimb.2021.686479](https://doi.org/10.3389/fcimb.2021.686479)
- [69] Aas JA, Paster BJ, Stokes LN, et al. Defining the normal bacterial flora of the oral cavity. *J Clin Microbiol.* 2005;43(11):5721–5732. doi: [10.1128/JCM.43.11.5721-5732.2005](https://doi.org/10.1128/JCM.43.11.5721-5732.2005)
- [70] Abusleme L, Dupuy AK, Dutzan N, et al. The subgingival microbiome in health and periodontitis and its relationship with community biomass and inflammation. *Isme J.* 2013;7(5):1016–1025. doi: [10.1038/ismej.2012.174](https://doi.org/10.1038/ismej.2012.174)
- [71] Stingu CS, Eschrich K, Rodloff AC, et al. Periodontitis is associated with a loss of colonization by *streptococcus sanguinis*. *J Med Microbiol.* 2008;57(4):495–499. doi: [10.1099/jmm.0.47649-0](https://doi.org/10.1099/jmm.0.47649-0)